Double Periodic Lamellar-in-Lamellar Structure in Multiblock Copolymer Melts with Competing Length Scales

Rikkert Nap,[†,‡] Nazar Sushko,[†] Igor Erukhimovich,[§] and Gerrit ten Brinke*,[†]

Department of Polymer Chemistry and Materials Science Centre, University of Groningen, Nijenborgh 4, 9747 AG Groningen, The Netherlands; Department of Chemistry, Purdue University, 560 Oval Drive, West-Lafayette, Indiana 47907; and Chair of Physics of Polymers and Crystals, Physics Department, Moscow State University, Leninskie Gory 119992 Moscow, Russia

Received June 2, 2006; Revised Manuscript Received July 18, 2006

ABSTRACT: The results of a detailed theoretical investigation of the phase behavior of A_m-*b*-(B-*b*-A)$_n$ multiblock copolymer melts are presented for the special case of $m = 20$ and $n = 10$. The presence of two strongly different molecular length scales results in the formation of a large-length-scale lamellar structure of alternating A_{20} and (B-*b*-A)$_{10}$ layers on cooling. On further cooling, the (B-*b*-A)$_{10}$ layers subsequently transform internally into small-length-scale layers of the A and B blocks: a lamellar-in-lamellar morphology. The final structure consists of an alternation of one "thick" layer and seven "thin" layers and compares favorably with recent experimental results of Matsushita and co-workers on slightly different systems.

1. Introduction

Structure formation in simple AB block copolymer melts usually involves only one characteristic length scale. More complex morphologies involving multiple length scales can be found in simple triblock copolymer systems with more than two monomer types.[1−5] Another possibility to produce complex structures is by using more complicated copolymer architectures as in the experiments by Ikkala and Ten Brinke and co-workers.[6−8] They found hierarchical two-length-scale structure-in-structure morphologies for a polystyrene-*block*-poly(4-vinylpyridine) (PS-*b*-P4VP) diblock copolymer with side chains (e.g., pentadecylphenol, PDP) attached by hydrogen bonds to the P4VP block. These linear-comb diblock copolymers show typical two-length-scale hierarchical structure-in-structure morphologies. First, the linear blocks microphase separate from the comb blocks, giving rise to the well-known classical morphologies. This morphology depends on the volume fraction of the blocks and corresponds to the large length scale. An additional short-length-scale lamellar ordering occurs inside the comb P4VP(PDP) domains at temperatures below ca. 60 °C. The structure-in-structure formation of these comb-shaped supramolecules can be used to manufacture functional materials with interesting electronic and photonic properties due to the strong temperature sensitivity of the hydrogen bonds defining the side-chain character of the comb blocks.[6,9] Because of the presence of three chemically different moieties, the occurrence of such two-length-scale structure-in-structure morphologies is not really surprising once the short-length-scale structure formation of the side-chain polymer is known. However, the question arises whether the presence of three chemically different species is really essential to obtain hierarchically two-length-scale ordered self-assembled materials.

To address this, in a number of papers the self-assembly of block copolymer systems involving only two chemically different species, but with a characteristic two-length-scale molecular architecture, was investigated.[10−16] One of the simplest systems considered consisted of an A_m-*b*-(B-*b*-A)$_n$ multiblock copolymer where a (B-*b*-A)$_n$ multiblock copolymer is covalently linked to a homopolymer A_m block. Here both A and B represent chemically different "short" chain molecules (Figure 1).

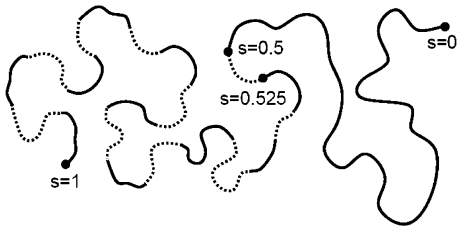

Figure 1. Schematic representation of A_m-*b*-(B-*b*-A)$_n$ molecule with $m = 20$ and $n = 10$. The numbers indicate monomers positions used in the Results and Discussion section.

This model is a seemingly drastic simplification of the comb-shaped supramolecules system described above; however, it preserves the essential feature of the latter, in principle being able to microphase separate at two different length scales. The first "large" length scale corresponds to microphase separation between the A_m block and the (B-*b*-A)$_n$ multiblock, while the second one involves microphase separation between the chemically different units that make up the A and B blocks of the (B-*b*-A)$_n$ multiblocks.[12] In the present paper we turn our attention once more to this system. Using more advanced numerical methods, we observe that, in contrast to our previous findings,[12] structure-in-structure morphologies occur in a most natural way. This result is in excellent agreement with recent findings of Matsushita and co-workers,[17] who observed a lamellar-in-lamellar structure for PS-*b*-(PI-*b*-(PS-*b*-PI)$_4$)-*b*-PS multiblock copolymer consisting of two polystyrene (PS) end blocks of considerable higher molar mass than the 4 (polystyrene) and 5 (polyisoprene (PI)) blocks that form the multiblock copolymer middle block PI-*b*-(PS-*b*-PI)$_4$.

The remainder of this paper is organized as follows. In section 2 we briefly describe the theory and give an outline of the numerical methods used. Subsequently, the results are presented and discussed in sections 3 and 4.

2. SCMFT Theory and Its Numerical Implementation

The behavior of linear-alternating block copolymers is analyzed in the framework of the self-consistent mean-field

† University of Groningen.
‡ Purdue University.
§ Moscow State University.
* Corresponding author. E-mail: g.ten.brinke@rug.nl.

10.1021/ma061233z CCC: $33.50 © 2006 American Chemical Society
Published on Web 08/17/2006

theory (SCMFT). This theory has proven itself to be quite powerful and successful in describing the phase behavior of block copolymer melts. For a more detailed description of SCMFT for block polymers, see e.g. refs 18−20. In the present work we employ this theory to investigate a monodisperse melt of n_p multiblock copolymers. These multiblock copolymers, which we denote further as A_m-*b*-(B-*b*-A)$_n$, consist of a long homopolymer A_m block connected to a (B-*b*-A)$_n$ multiblock of *n* identical diblock repeat units. Here A and B represent themselves "short" chain molecules. In the present case, the A and the B blocks are assumed to have equal degrees of polymerization, which we denote as *d*. The length of the long linear block, expressed in units of *d*, is *m*. Consequently, the total length of the multiblock copolymer is $N = (2n + m)d$.

The basic ideas of the SCMFT include the following assumptions. The distribution of the polymer conformations is assumed to be Gaussian. The interactions or chemically incompatibility between chemically distinct monomers is described by the Flory−Huggins $\chi_{\alpha\beta}$ parameters. The melt is assumed to be incompressible, and the volumes $(1/\rho_0)$ of the different monomer types are identical. Taking into account all these assumptions, the free energy functional *F* reads[19]

$$\frac{F}{n_p kT} = \frac{F}{kT}\frac{N}{V\rho_0} = -\ln Q + \frac{1}{V}\int d\mathbf{r}\left[\sum_{\alpha\neq\beta}\frac{1}{2}\chi_{\alpha\beta}N\Phi_\alpha\Phi_\beta - \sum_\alpha W_\alpha\Phi_\alpha - \Xi\left(1 - \sum_\alpha \Phi_\alpha\right)\right] \quad (1)$$

where the functional $Q = \int D\mathbf{r}P[\mathbf{r};0,1]\exp[-\int_0^1 ds\,\sum_\alpha \sigma_\alpha(s)W_\alpha[\mathbf{r}(s)]]$ is the partition function of a single polymer chain in the external fields W_α. In eq 1, the monomer density functions are denoted by Φ_α and the Lagrange multiplier Ξ ensures the incompressibility. The function $P[\mathbf{r};0,1]$ describes the (Gaussian) conformational distribution function of the polymer chain.

The mean-field free energy $F[\phi_\alpha,\phi_\beta,w_\alpha,w_\beta,\xi]$ is determined by the saddle point of the free energy functional of eq 1,[19,20] which is given by the following set of equations:

$$w_\alpha(\mathbf{r}) = \sum_{\beta\neq\alpha}\chi_{\alpha\beta}N\phi_\beta(\mathbf{r}) + \xi(\mathbf{r}) \quad (2)$$

$$\phi_\alpha(\mathbf{r}) = -V\frac{\delta \ln Q}{\delta w_\alpha(\mathbf{r})} = \frac{V}{Q}\int_0^1 ds\,\sigma_\alpha(s)\,q(\mathbf{r},s)\,\bar{q}(\mathbf{r},s) \quad (3)$$

$$1 = \sum_\alpha \phi_\alpha(\mathbf{r}) \quad (4)$$

where $q(\mathbf{r},s)$ and $\bar{q}(\mathbf{r},s)$ are the end-segment distribution functions and $\sigma_\alpha(s)$ defines the architecture of the polymer; i.e., this function is unity if monomer *s* is of type α and zero otherwise. The variable *s* is proportional to the arc length along the contour of a polymer and enumerates the monomers. This variable ranges from 0 to 1 (see also Figure 1). The end-segment distribution function is the probability to find monomer *s* at position **r** independently of its starting position, and it satisfies a modified diffusion equation

$$\frac{\partial q(\mathbf{r},s)}{\partial s} = \frac{1}{6}Na^2\nabla^2 q(\mathbf{r},s) - w(\mathbf{r},s)\,q(\mathbf{r},s) \quad (5)$$

with an initial condition $q(\mathbf{r},0) = 1$ and external field $w(\mathbf{r},s) = \sum_\alpha \sigma_\alpha w_\alpha(\mathbf{r})$. Similarly, the second end-segment distribution function $\bar{q}(\mathbf{r},s)$ also satisfies a modified diffusion equation

$$-\frac{\partial \bar{q}(\mathbf{r},s)}{\partial s} = \frac{1}{6}Na^2\nabla^2\bar{q}(\mathbf{r},s) - w(\mathbf{r},s)\,\bar{q}(\mathbf{r},s) \quad (6)$$

with the initial condition $\bar{q}(\mathbf{r},1) = 1$. This end-segment distribution function is the probability to find monomer *s* at position **r** independently of its ending position. The partition function *Q* can be expressed in terms of the end-segment distribution function as follows: $Q = \int d\mathbf{r}\; q(\mathbf{r},1)$. An important quantity related to the end-segment distribution function is the monomer distribution function, which is defined as[21−23]

$$\rho(\mathbf{r},s) = \frac{V}{Q}q(\mathbf{r},s)\,\bar{q}(\mathbf{r},s) \quad (7)$$

An iteration scheme is used to solve the self-consistent field equations (2)−(6). The central issue in the iteration procedure is to solve the partial differential equations (5) and (6) for $q(\mathbf{r},s)$ and $\bar{q}(\mathbf{r},s)$ and calculate the densities using expression (3). In the present paper we use spectral as well as real-space methods to solve these diffusion equations. The spectral method, developed by Matsen and Schick,[19] has been highly successful in establishing the phase behavior of numerous block copolymer systems because it allows the accurate calculation of the free energy for any given complex morphology. In the spectral method the self-consistent-field equations are re-formulated in Fourier space, implying that every spatial depended function is expanded around a set of symmetry-dependent basis functions $f(\mathbf{r}) = \sum_i f_i\varphi_i(\mathbf{r})$. These basis functions $\varphi_i(\mathbf{r})$ are eigenfunctions of the Laplace equation $\nabla^2\varphi_i(\mathbf{r}) = -\lambda_i/D^2\varphi_i(\mathbf{r})$, where the variable *D* corresponds to the periodicity of the structure under consideration. For example, the basis functions for the lamellar phase are

$$\varphi_i(z) = \begin{cases}\sqrt{2}\cos(2\pi(i-1)/D) & i \neq 1\\ 1 & i = 1\end{cases} \quad (8)$$

In Fourier space the partial differential equation turns into a first-order differential equation which can be solved in a straightforward manner. However, the spectral method has a number of disadvantages; e.g., it requires prior information about the symmetry of the structure as an input. But the major disadvantage, especially for complex copolymer architectures such as the ones considered in this paper, is the considerable computational effort required to compute the polymer volume fraction. The number of function evaluations in eq 3 per iteration cycle needed for the multiblock copolymers considered here scales with the number of basis functions N_r as $O(N_r^6)$, whereas for a diblock copolymer system it scales only as $O(N_r^4)$. Consequently, this complicates calculations for higher degrees of segregation, i.e., larger values of χ, due to the large number of basis functions required to obtain an accurate solution.

To explore also stronger segregations, we employ a real-space method. We discretize both the spatial and the contour coordinates and use a Crank−Nicolson numerical algorithm[23] with "reflecting" boundary conditions to solve the modified diffusion equation. The Crank−Nicolson algorithm is combined with the unit cell approximation (UCA).[25−27] Within this approximation we are only able to examine symmetries in lamellar, cylindrical, and spherical coordinate systems. A real-space approach combined with the UCA approximation requires only $O(N_rN_s)$ calculations per iteration cycle, where N_s is the number of chain contour steps and N_r the number of spatial steps. Note that the number of spatial steps is equivalent to the number of basis functions. Typically we use $N_s/(2n + m) = 500$ and $N_r = 100-300$. With the spectral method we are

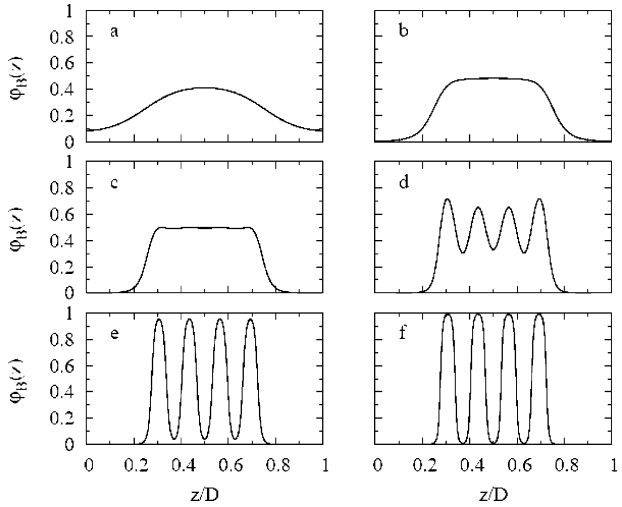

Figure 2. Density profiles of B-type monomers ordered into lamellar structures as a function of $\chi d = 1.25$, 2.5, 4.5, 7.5, 12.5, and 20. The spatial coordinate z is expressed in units of the domain size D.

restricted to $N_r = 30-40$. The amount of computational time shows that at least for the present multiblock copolymers the real-space method combined with the UCA approximation is preferable over the spectral method. Using a general 3D real-space approach would not be beneficial as this leads to a substantial increase in the number of computations per iteration cycle, namely $O(N_r^3 N_s)$, and in the number of self-consistent equations to be solved.

A third approach for solving partial differential equations is a pseudo-spectral method developed by Rasmussen and Kalosakas for block copolymers.[28] It is a potentially powerful method because it does not require any prior information about the symmetry like any 3D real-space method. So far we have used this method only in one and two dimensions for a number of test cases to validate the computations performed within the other two approaches.

We employ various iteration schemes to solve the self-consistent equations: the Broyden algorithm, simple, and Anderson mixing methods.[29−31] Having obtained a solution of the SCMFT equations (2)−(6), one can calculate the free energy, which subsequently is minimized with respect to the periodicity D. The equilibrium state is obtained by comparing the free energies of different structures and selecting the structure with minimal free energy.

3. Results and Discussion

We consider multiblock copolymer as A_{20}-*b*-(B-*b*-A)$_{10}$, where the number of units of the (B-*b*-A)$_{10}$ multiblock equals the number of units of the homopolymer A_{20} block. The number of B-*b*-A diblock copolymers has been chosen to be relatively large to enhance the difference between the two length scales involved. Because of the architecture, the phase behavior of the copolymer melt resembles that of diblock copolymers close to the order−disorder transition (ODT); i.e., segregation occurs between the homopolymer A_{20} block and the (B-*b*-A)$_{10}$ multiblock. Therefore, not surprisingly, a symmetric lamellar structure is the equilibrium morphology at the ODT.[11,12] However, far from the ODT a deviation from diblock-like phase behavior is anticipated, and lamellar-in-lamellar morphologies become feasible.

To discuss the structure development, we present in Figure 2 a number of density profiles at different stages of separation, showing the evolution of the lamellar phase. Just below the ODT we observe a weakly segregated lamellar structure with the same periodicity as found in diblock copolymer systems with a degree of polymerization $N = 2n + m$ (see Figure 2a). This is a clear indication that the A_{20} blocks segregate spatially from the (B-*b*-A)$_{10}$ multiblocks. The A-rich layers contain more A_{20} blocks, whereas the amount of (B-*b*-A)$_{10}$ multiblocks is larger in the B-rich domains. Upon cooling, the A-rich domains become pure and contain essentially only A_{20} blocks. However, within the B-rich domains the A- and B-block monomers of the (B-*b*-A)$_{10}$ multiblocks remain homogeneously mixed (see Figure 2b). On further decreasing the temperature, the A and B monomers of the (B-*b*-A)$_{10}$ multiblocks segregate from each other, and a lamellar-in-lamellar structure appears as can be concluded from the density profiles in Figure 2c−e. The last density profile (Figure 2f) shows a strongly separated lamellar-in-lamellar structure at high χ values. A cartoon of the self-assembled large-length-scale lamellar structure for $\chi d = 2.5$ (Figure 2b) and the lamellar-in-lamellar structure for $\chi d = 12.5$ (Figure 2e) is presented in Figure 3.

Figure 4 shows the development of the lamellar periodicity upon cooling. Initially the periodicity follows that of a diblock copolymer melt. However, whereas the domain spacing of a diblock melt increases monotonically with decreasing temperature, the periodicity of the linear-alternating multiblock copolymer melt passes through a local maximum. This interesting feature occurs at $\chi d \cong 7$. A reduction in domain spacing occurs after the appearance of the secondary lamellar domains. The large domains are influenced by the small domains and vice versa. Indeed, the size of the large domains has to be commensurate with the size of the small domains since the harmonics forming the profile of the small domains also have to satisfy the periodicity conditions for the large domains. To make the comparison with a diblock copolymer, we introduced an effective χ parameter for the latter defined as $\chi_{\text{eff}} = \chi/4$. The factor 1/4 arises from the reduction of interaction strength in the A_{20}-*b*-(B-*b*-A)$_{10}$ multiblock copolymer compared to diblock copolymers. The effective Flory−Huggins parameter for a mixture of A_{20} homopolymers and (B-*b*-A)$_{10}$ multiblock copolymers is reduced by a factor 1/4 compared to a mixture of e.g. A_{20} and B_{20} homopolymers.

Figure 5 shows the free energy landscape of the lamellar phase at $\chi d = 12.5$ as a function of the domain spacing D. Each minimum in Figure 5 corresponds to a different density profile presented in Figure 6, where each density profile has a different number of small AB domains. The free energy landscape has many local minima. The difference between them is rather small; e.g., the difference between local minimum (e) and the global minimum (d) is only about 3%.

In Figure 7 the domain spacing vs χ for the stable as well as the metastable lamellar structure is depicted. The different branches appear to emanate from a region located at $\chi d = 7.5$. The evolution of the single lamellar structure appears to be continuous up to $\chi d = 7.5$, where the transition between single periodic lamellar and the double periodic lamellar-in-lamellar really occurs. The nature of this transition is further examined in Figure 8, presenting the free energy and the internal energy vs the χ value. The figure shows that the free energy and the internal energy as well as their derivatives have no discontinuities. Consequently, the transition cannot be classified as a first-order phase transition. We conjecture that it is either a continuous transition or a crossover behavior. The second microphase separation or the appearance of the secondary structure takes place in finite-sized domains where no sharp transitions occur. Hence, it is not surprising that a smooth

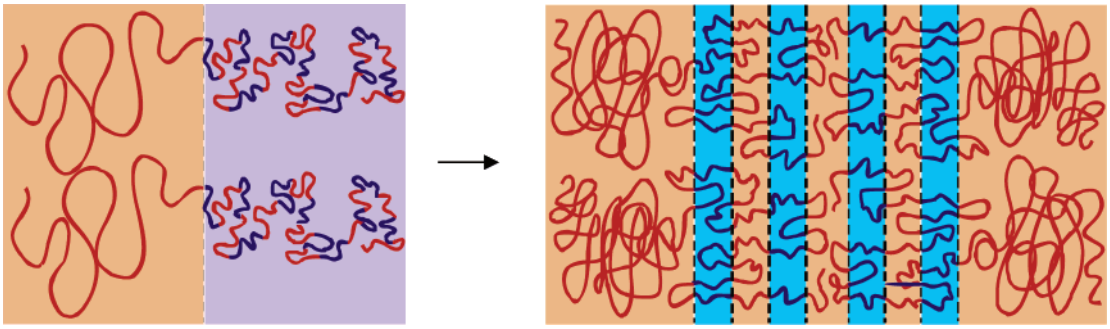

Figure 3. Schematic illustration of the "large-length-scale" lamellar structure at $\chi d = 2.5$ and the formation of the lamellar-in-lamellar structure on further cooling to e.g. $\chi d = 12.5$.

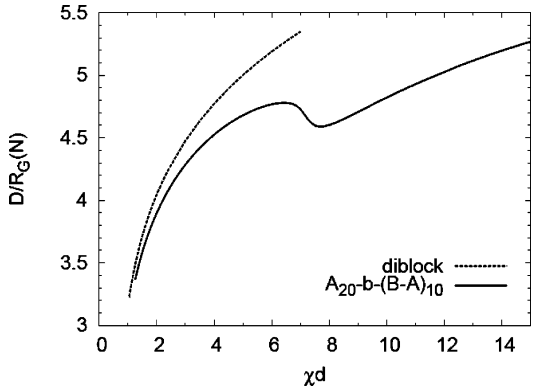

Figure 4. Period D as a function of χd for the lamellar structure of the A_{20}-*b*-$(B$-*b*-$A)_{10}$ multiblock copolymer. D is expressed in units of the radius of gyration $R_G(N) = \sqrt{N/6}a$. Shown are results for A_{20}-*b*-$(B$-*b*-$A)_{10}$ as well as for a regular diblock copolymer.

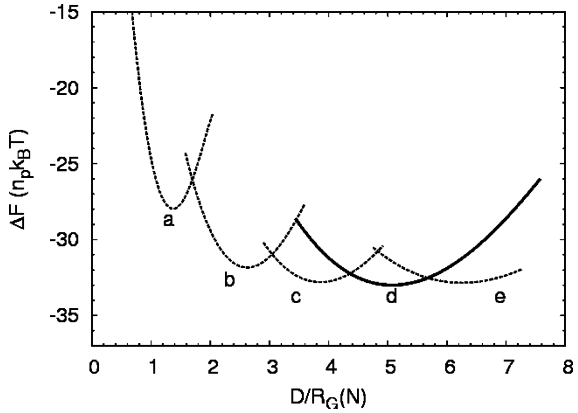

Figure 5. Free energy difference ΔF as a function of the domain spacing D for $\chi d = 12.5$. The letters indicate local minima. Situation d corresponds to the global minimum.

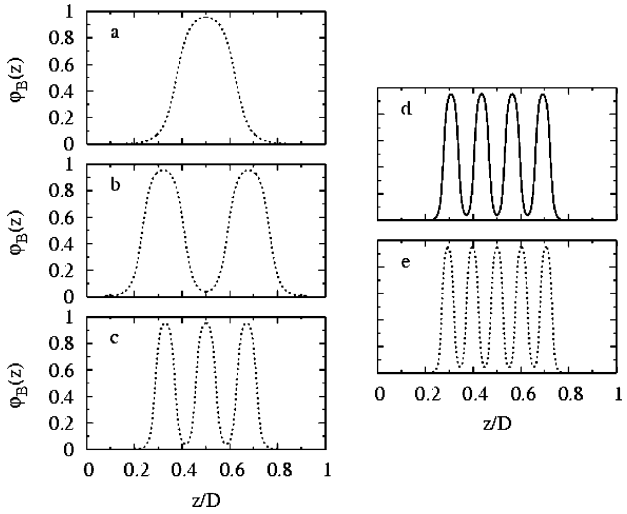

Figure 6. Density profiles of B-block monomers ordered in lamellar structures at $\chi d = 12.5$ belonging to the different local minima of the free energy. The letters correspond to the local minimum of the free energy presented in Figure 5. Case d is the equilibrium density profile.

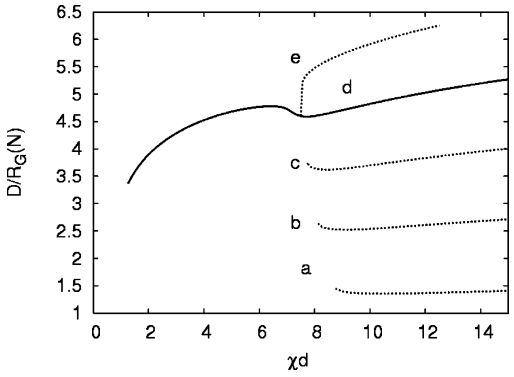

Figure 7. Period D as a function of χd for the lamellar structure of the A_{20}-*b*-$(B$-*b*-$A)_{10}$ multiblock copolymer for the global minimum (solid line) as well as the local minima (dashed lines). D is expressed in units of the radius of gyration $R_G(N) = \sqrt{N/6}a$. Note that it proved numerically difficult to establish the point(s) where the metastable structures first appear exactly.

crossover behavior is observed. Note also that a smooth change in the slope of the internal energy, i.e., heat capacity, occurs for $\chi d \cong 7.5$. This change can be attributed to the fact that the double periodic lamellar-in-lamellar structure has a different heat capacity as the single periodic lamellar structure. It takes place in the same region of χ values as the occurrence of the local maximum in the domain spacing and the appearance of the metastable structures.

As can be seen from the density profile in Figure 2e, the internal morphology is quite complex. To obtain more detailed information about the conformations, we calculated the monomer distribution functions. Figure 9 shows this function for various values of the monomer position s together with the equilibrium density profile for the separation given by $\chi d = 12.5$. We observe that the distribution function for $s = 0.5$, which corresponds to the junction point between the homopolymer block and the alternating multiblock, is sharply peaked around the interface. This implies that the homopolymer blocks are well separated from the alternating multiblocks. The distribution function for $s = 0.525$, or in other words the first junction between two consecutive A and B blocks of the alternating multiblocks, shows a bimodal distribution, proving that a significant number of the first alternating blocks forms a looped conformation. Finally, the distributions of the first and the last monomers, $s = 0$ and $s = 1$, are presented. The first A

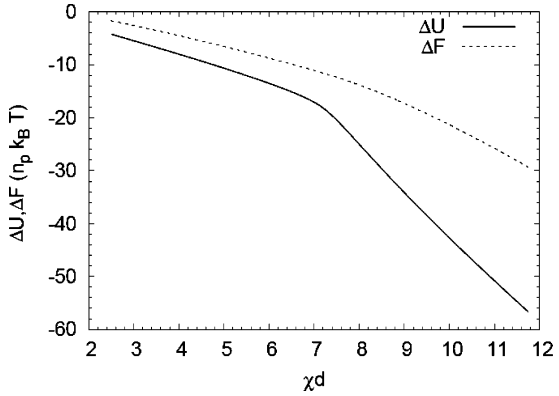

Figure 8. Difference ΔF between the free energy of the lamellar and the disordered phase and the difference ΔU between internal energy of the lamellar and the disordered phase as a function of χd. Both energies are expressed in units of $n_p k_B T$.

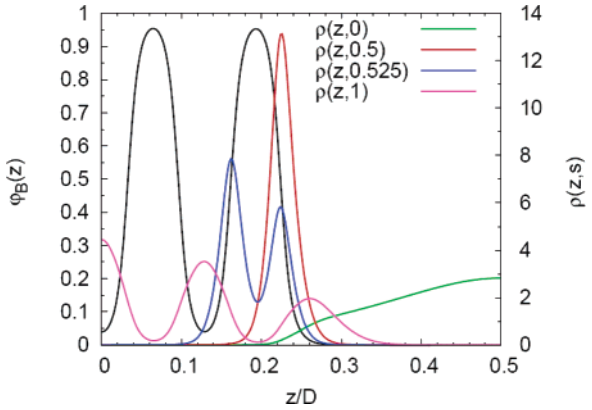

Figure 9. Monomer distribution function $\rho(z,s)$ for $\chi d = 12.50625$ for different values of monomer positions s, namely $s = 0.5$, $s = 0.525$, $s = 1$, and $s = 0$. Also shown in black is the B-block monomer density profile. The results are only presented for half of the domain due to symmetry.

monomer is located throughout the larger domain, while the last monomer appears only in every small A-rich domain, showing a large asymmetry in the conformation of the chain.

For the entire χ value range under consideration we also calculated the free energy for other morphologies, notably the cylindrical and spherical phases in the real space approach and hexagonal and body-centered cubic and simple cubic phases in the spectral approach. The lamellar phase was always found to have the lowest free energy. Finally, to safeguard that we did not overlook any novel unexpected structures, we also applied the pseudo-spectral algorithm. A number of test calculations in one and two dimensions were performed, and so far we did not find structures having a lower free energy then the lamellar morphology. In this respect it is not without interest to note that, as already mentioned in the Introduction, recently Matsushita and co-workers observed a lamellar-in-lamellar ordered morphology for PS-*b*-(PI-*b*-(PS-*b*-PI)$_4$)-*b*-PS multiblock copolymers consisting of two polystyrene (PS) end blocks of considerable higher molar mass than the polystyrene and polyisoprene (PI) blocks that form the PI-*b*-(PS-*b*-PI)$_4$ middle multiblock.[17] In this case alternating "thick" PS layers and layers of similar thickness consisting of three alternating "thin" PI, PS, and PI layers were found. In a related system of PISISISISIP undecablock terpolymer consisting of two poly(2-vinylpyridine) (P) end-blocks that are longer than the alternating polyisoprene (I) and polystyrene (S) blocks that form the middle multiblock, a lamellar-in-lamellar structure was found with "thick" P layers alternated with five thin I−S−I−S−I layers.[32]

4. Concluding Remarks

In this paper we presented a detailed analysis of a microphase separation in a specific multiblock copolymer system consisting of macromolecules with a molecular architecture involving two vastly different length scales. Advances made in the numerical implementation allowed us to examine the structure-in-structure development. At elevated temperatures a diblock-like phase separation was found, whereas upon reducing the temperature a lamellar-in-lamellar appeared. This latter structure combines properties of multiblock and diblock copolymers.

A theoretically important observation is that the investigation of self-assembly in systems containing complex copolymer architectures requires more advanced numerical approaches.[31] We believe that the pseudo-spectral method[28] might be an appropriate tool and are currently applying this method to our block copolymer systems. Furthermore, we are extending the analysis to related block copolymers system, such as the multiblock copolymers A$_m$-*b*-(B-*b*-A)$_n$-B$_k$, for which the weak segregation behavior has been already addressed theoretically,[15] and the A$_m$-*b*-(B-*b*-A)$_n$-*b*-B-*b*-A$_m$ multiblock copolymers studied experimentally by Matsushita and co-workers.[17] If both end-blocks have equal length, i.e., $m = k$, the former class of multiblock copolymers lends itself particularly well for a weak segregation Landau free energy approach, since due to the symmetry all order−disorder transitions occur at a critical point. In refs 13 and 15, these multiblock copolymer systems were shown to exhibit very rich phase behavior. Depending on the relative length of the end-blocks, the weak-segregated structures range from "short-length-scale" lamellar to simple cubic to face-centered cubic to single gyroid to "large-length-scale" lamellar. The present A$_m$-*b*-(B-*b*-A)$_n$ multiblock copolymer system, only investigated here for $m = 20$ and $n = 10$, is likewise expected to exhibit very rich phase behavior. A systematic experimental study of either of these systems would be very helpful. In this respect it is important to realize that such a study does not necessarily require that many B-*b*-A repeat diblock copolymers. In the present study $n = 10$ was merely selected to create a large difference in the two length scales involved.

Acknowledgment. The authors gratefully acknowledge the Netherlands Scientific Organization for supporting this work as part of the Dutch Russian Research Cooperation Program 2003 (NWO Grant 047.016.002).

References and Notes

(1) Breiner, U.; Krappe, U.; Thomas, E. L.; Stadler, R. *Macromol. Chem. Phys.* **1997**, *198*, 1051.
(2) Breiner, U.; Krappe, U.; Thomas, E. L.; Stadler, R. *Macromolecules* **1998**, *31*, 135.
(3) Hamley, I. W. *The Physics of Block Copolymers*; Oxford University Press: Oxford, 1998.
(4) Bates, F. S.; Fredrickson, G. H. *Phys. Today* **1999**, *52*, 32.
(5) Abetz, V.; Simon, P. F. W. *Adv. Polym. Sci.* **2005**, *189*, 125.
(6) Ruokolainen, J.; Mäkinen, R.; Torkkeli, M.; Mäkelä, T.; Serimaa, R.; Ten Brinke, G.; Ikkala, O. *Science* **1998**, *280*, 557.
(7) Ruokolainen, J.; Ten Brinke, G.; Ikkala, O. *Adv. Mater.* **1999**, *11*, 777.
(8) Ikkala, O.; Ten Brinke, G. *Science* **2002**, *295*, 2407.
(9) Valkama, S.; Kosonen, H.; Ruokolainen, J.; Torkkeli, M.; Serimaa, S.; Ten Brinke, G.; Ikkala, O. *Nat. Mater.* **2004**, *3*, 872.
(10) Nap, R.; Kok, C.; Ten Brinke, G.; Kuchanov, S. I. *Eur. Phys. J. E* **2001**, *4*, 515.
(11) Nap, R.; Ten Brinke, G. *Macromolecules* **2002**, *35*, 952.
(12) Nap, R.; Erukhimovich, I. Y.; Ten Brinke, G. *Macromolecules* **2004**, *37*, 4296.
(13) Smirnova, Y. G.; Ten Brinke, G.; Erukhimovich, I. Y. *Polym. Sci. Ser. A* **2005**, *47*, 430.
(14) Pichugin, V. E.; Kuchanov, S. I. *J. Stat. Mech.* **2005**, P07009.

(15) Smirnova, Y. G.; Ten Brinke, G.; Erukhimovich, I. Y. *J. Chem. Phys.* **2006**, *124*, 0544907.
(16) Kuchanov, S. I.; Pichugin, V.; Ten Brinke, G. *e-Polym.* **2006**, 012.
(17) Nagayata, Y.; Masuda, J.; Noro, A.; Cho, D.; Takano, A.; Matsushita, Y. *Macromolecules* **2005**, *38*, 10220.
(18) Schmid, F. *J. Phys.: Condens. Matter* **1998**, *10*, 8105.
(19) Matsen, M. W.; Schick, M. *Phys. Rev. Lett.* **1994**, *72*, 2660.
(20) Fredrickson, G.; Ganesan, V.; Drolet, F. *Macromolecules* **2002**, *35*, 16.
(21) Rasmussen, K. Ø.; Kober, E. M.; Lookman, T.; Saxena, A. *J. Polym. Sci., Part B: Polym. Phys.* **2003**, *41*, 104.
(22) Matsen, M.W. *J. Chem. Phys.* **1995**, *102*, 9698.
(23) Matsen, M. W.; Thompson, R. B. *J. Chem. Phys.* **1999**, *111*, 7139.
(24) Mitchell, A. R.; Griffiths, D. F. *The Finite Difference Method in Partial Differential Equations*; John Wiley and Sons: Chichester, 1980.
(25) Helfand, E.; Wasserman, Z. R. *Macromolecules* **1978**, *11*, 960.
(26) Helfand, E.; Wasserman, Z. R. *Macromolecules* **1980**, *13*, 994.
(27) Vavasour, J. D.; Whitmore, M. D. *Macromolecules* **1992**, *25*, 5477.
(28) Rasmussen, K. Ø.; Kalosakas, G. J. *Polym. Sci., Part B: Polym. Phys.* **2002**, *40*, 1777.
(29) Thompson, R. B.; Rasmussen, K. Ø.; Lookman, T. *J. Chem. Phys.* **2004**, *120*, 31.
(30) Eyert, V. *J. Comput. Phys.* **1996**, *124*, 271.
(31) Ceniceros, H. D.; Fredrickson, G. H. *Multiscale Model. Simul.* **2004**, *2*, 452.
(32) Masuda, J.; Nagata, Y.; Noro, A.; Takano, A.; Matsushita, Y. *Phys. Rev. Lett.*, in press.

MA061233Z